Optical-phonon emission in GaAs/AlAs multiple-quantum-well structures determined by hot-electron luminescence

V. F. Sapega
Max-Planck-Institut für Festkörperforschung, Heisenbergstrasse 1, D70569 Stuttgart, Germany and A. F. Ioffe Physical-Technical Institute, St. Petersburg 194021, Russia

M. P. Chamberlain, T. Ruf, and M. Cardona
Max-Planck-Institut für Festkörperforschung, Heisenbergstrasse 1, D70569 Stuttgart, Germany

D. N. Mirlin
A. F. Ioffe Physical-Technical Institute, St. Petersburg 194201, Russia

K. Tötemeyer, A. Fischer, and K. Eberl
Max-Planck-Institut für Festkörperforschung, Heisenbergstrasse 1, D70569 Stuttgart, Germany
(Received 9 June 1995)

We have performed hot-electron photoluminescence experiments on a number of different Be-doped GaAs/AlAs multiple-quantum-well structures (MQW's), with fixed well width of 40 Å and barrier thicknesses between 5 and 80 Å, in order to determine the energy of the optical phonons emitted by the hot electrons before recombination with the acceptor levels of the GaAs quantum wells. A continuum theory of optical phonons in GaAs/AlAs multiple quantum wells was used to estimate the effective energy of the optical phonons emitted during the hot-electron energy relaxation. The theoretical calculations are compared with the energy separation of the measured hot photoluminescence peaks and a detailed analysis of the different modes contributing to the energy relaxation is performed. For MQW's with large barriers, i.e., 40-Å GaAs and 80 Å AlAs, the energy relaxation is dominated by the AlAs phonons. However, for samples with smaller barrier widths, i.e., 40-Å GaAs and either 5- or 10-Å AlAs, relaxation via the emission of GaAs modes is more important. Nevertheless, relaxation by AlAs phonons is still significant producing an *effective* energy separation of the hot photoluminescence peaks between that of the pure GaAs and the AlAs MQW optical-phonon energies.

I. INTRODUCTION

It has been known for several years that the radiative recombination of electrons with neutral acceptors, during hot-electron photoluminescence, can be used to study photoexcited carriers.[1] This technique has been applied to investigate a number of different phenomena including hot-electron relaxation,[2–4] valence band structure,[5–7] and the interaction of electrons with coupled phonon plasmons.[8]

There has been a vast number of theoretical treatments, which consider optical phonons in quantum wells and superlattices and their interaction with electrons. For example, the microscopic *ab initio* calculations of Baroni et al.[9,10] have been shown to describe well the experimental dispersion relations of bulk GaAs (Ref. 11) and AlAs.[12] Force constants from calculations for the bulk have been used, mainly within the mass approximation, to evaluate the optical-phonon modes of GaAs/AlAs superlattices. A continuum model of optical phonons in multiple-quantum-well (MQW) structures has also been developed, which treats fully the mixing between longitudinal, transverse and *interface* components.[13] It is in good agreement[13] with the *ab initio* results mentioned above and describes extremely well the angular dispersion of optical phonons in $(GaAs)_8(AlAs)_8$ and $(GaAs)_{12}(AlAs)_{12}$ superlattices, which have been determined experimentally by micro-Raman scattering.[14] Furthermore, it has been used to calculate resonant Raman spectra[15,16] in GaAs/AlAs MQW's, where the phonon wave vectors are induced via interface roughness scattering, and to analyze non-resonant Raman spectra[17] in similar structures where crystal momentum conservation with the incoming and scattered light determines the phonon wave vectors.

The relaxation of hot electrons in MQW's via optical-phonon emission has also been extensively investigated. The importance of the role of AlAs interface modes with decreasing GaAs well width was demonstrated by time-resolved Raman scattering measurements.[18] More comprehensive time-resolved Raman studies considered the well width dependence of the electron relaxation[19] and made favorable comparisons for the occupation numbers of the different confined and *interface* phonons with the model of Huang and Zhu.[20] The importance of the AlAs *interface* modes was also shown by hot-electron photoluminescence and high temperature mobility measurements in the $GaAs/Ga_xAl_{1-x}As$ system.[21] Recently, hot-electron photoluminescence has been used to consider

0163-1829/95/52(19)/14144(6)/$06.00

electron relaxation in different GaAs/AlAs MQW structures with a fixed barrier width of 100 Å and well widths varying from 40 to 130 Å.[22] It was shown that the relaxation of electrons in the GaAs layers is dominated by GaAs phonons for the larger wells, but by AlAs phonons for the 40 Å GaAs well width sample.

In this work, we use hot-electron photoluminescence to investigate the relaxation of electrons in GaAs/AlAs samples, where the well width is fixed at 40 Å and the AlAs width varies from 5 to 80 Å , covering the transition from superlattices to multiple quantum wells. We analyze the results considering energy relaxation of electrons by phonons calculated within the continuum theory,[13] which has been so successful in analyzing Raman scattering experiments in GaAs/AlAs MQW's.

II. LUMINESCENCE SPECTRA

The samples investigated were grown by molecular-beam epitaxy on (100)-oriented undoped semi-insulating GaAs substrates kept at 580° C. The central regions (≈ 15 Å) of the GaAs layers were doped with Be, while the edges of these layers (≈ 12 Å) were left undoped. The sample parameters, listed in Table 1, were determined by double-crystal x-ray diffraction, using Cu $K\alpha_1$ radiation and by Hall-effect measurements.

For the excitation of hot-electron photoluminescence (HPL), a dye-laser (R6G) pumped by an Ar^+-ion laser was used. The samples were mounted in an optical exchange-gas cryostat and kept at a temperature of 6 K. The HPL was analyzed by a SPEX 1404 double monochromator, equipped with a cooled GaAs photomultiplier and conventional photon-counting electronics.

Figure 1 shows the HPL spectra of the (40/80) Å, (40/34) Å, (40/14) Å, (40/5) Å GaAs/AlAs MQW samples. The excitation energy in all three cases was chosen to promote electrons into the conduction band with the same kinetic energy of ϵ_0=220 meV. To demonstrate the changes of the HPL spectra with AlAs thickness more clearly, they are plotted as a function of the energy of the electrons in the conduction band, with the "0" phonon peaks for all four samples adjusted to the same energy. All the spectra show an oscillatory dependence of the intensity with electron energy. The peak labeled "0" in each spectrum corresponds to recombination of electrons, from the state at which they were created, with a neutral acceptor. The inset in Fig. 1 shows the scheme of the optical transitions. The width of the "0" peak is determined by the electron energy distribution at the point of creation, which is related to heavy hole subband warping, as well as the energy distribution of acceptors, the final state of recombination for the hot photoluminescence process.[1] The width of this distribution has been estimated from the band gap luminescence as δ_A=20–25 meV. It is very close to the width of the "0" peak in the HPL spectra. This relatively narrow energy distribution of the acceptor levels arises from the controlled doping of the center of the GaAs layers and leads to well resolved hot luminescence spectra. The energy separation between the "0" and "1" peaks of the spectra is directly related to the loss mechanisms responsible for electron energy relaxation (see inset in Fig. 1). The power density of the laser used for the excitation of the spectra was 10–15 Wcm^{-2}, which resulted in a density of photocreated electrons between (1–1.5) × 10^9 cm^{-2}. As a consequence of this low electron density, the main mechanism of energy relaxation in the samples studied is the emission of optical phonons.[23] The separation of the "0" and "1" peaks in the spectra should allow one to determine the energy of the phonons, which can be in the GaAs and/or the AlAs reststrahl region. To determine the energy separation between the peaks in the energy distribution function more accurately, we divide the HPL spectrum by the distribution function,

$$\Phi(\epsilon) = [1 + \epsilon_c m_c/(E_A m_h)]^{-4}, \quad (1)$$

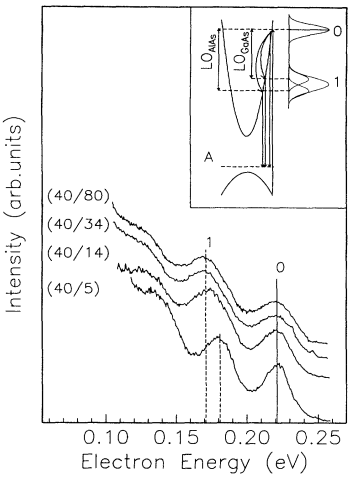

FIG. 1. Hot-electron photoluminescence spectra for four GaAs/AlAs MQW samples plotted as a function of the electron energy above the bottom of the confined quantum-well state. The vertical line labeled "0" is the zero-phonon energy peak corresponding to recombination at the energy of creation. The vertical dashed lines labeled "1" indicate the maximum positions of the peak after the emission of one optical phonon for the largest and smallest barrier widths. The inset shows schematically the creation of photoexcited electrons, their relaxation by emission of GaAs and AlAs MQW optical phonons, and the final step of recombination with an acceptor level (A).

TABLE I. Parameters of the GaAs/AlAs MQW samples used in the hot photoluminescence experiments.

Sample	GaAs width [Å]	AlAs width [Å]	Doping × 10^{18} cm^{-3}
40/5	39	5	1.0
40/9	40	9	0.8
40/14	38	14	1.3
40/20	40	20	0.8
40/34	40	34	1.0
40/80	40	80	0.7

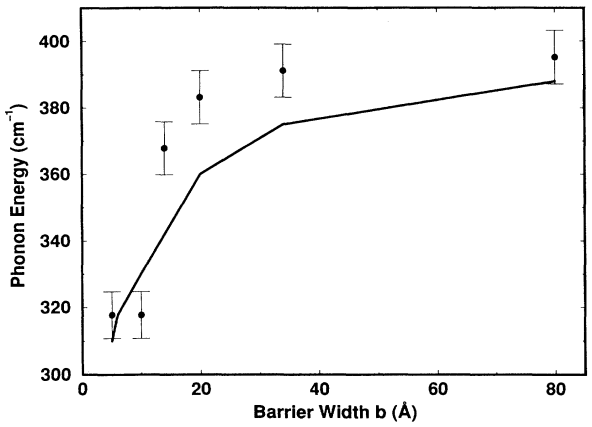

FIG. 2. Measured energy difference (dots) between the "0" and "1" phonon peaks in the hot photoluminescence spectra of GaAs/AlAs MQWs vs barrier width. The solid line is the calculated effective phonon energy of emission determined from the strength of the interaction of the GaAs and AlAs MQW phonons.

which describes the probability that an electron with energy ϵ will recombine with a hole bound to an acceptor[24]. In this formula, we used the experimental value of the acceptor binding energy of E_A=42 meV and m_c=0.11m_0 for the electron effective mass (including nonparabolicity[25]), and calculated in Ref. 24 for bulk acceptor mass m_h=0.66m_0. In order to determine the energy separation between the first two peaks, the energy spectra of the electrons were fitted by Gaussian distributions. The energy difference between the "0" and "1" peaks, including the uncertainty in their determination, is plotted for all the six samples as a function of barrier width in Fig. 2. For the samples with larger barrier widths, the energy of the emitted phonons approaches 395 cm^{-1}, a value in the AlAs phonon regime. For the smaller barrier widths, the energy of the emitted phonons decreases to about 320 cm^{-1}, which is above that of the GaAs phonons, but well below that of the AlAs modes. Figure 2 also depicts a theoretical curve (solid line), which will be discussed later.

III. ANALYSIS OF THE PHOTOLUMINESCENCE SPECTRA

To analyze the results in Fig. 2, we need to look at the process of electron-optical-phonon interaction in the GaAs/AlAs MQW's. We assume that due to the low density of photo-excited electrons, the main energy loss mechanism is the emission of pure optical phonons and that phonon-plasmon coupling is negligible. The initially excited electron states have an excess energy of 220 meV above the subband minimum. After the emission of a phonon of energy 37 meV the electron state has reduced its energy to 183 meV. This energy difference between the initial and final electron states assuming a parabolic conduction band, gives the minimum in-plane wave vector transferred to the optical phonon of $q_x \approx 5.2 \times 10^5$ cm^{-1}. This is calculated for the GaAs phonons, when a phonon energy of 50 meV is used for the AlAs phonons $q_x \approx 7.3 \times 10^5$ cm^{-1}. The optical phonons of the MQW's also have a phonon wave vector in the growth direction, q_z, that relates the phases of the phonon scalar potentials in subsequent periods of the structure. This phonon wave vector can take any value from 0 to $\pi/(a+b)$, where a and b are the widths of the GaAs and AlAs layers of the MQW, respectively.

In Fig. 3, we plot the dispersion of the optical phonons for a fixed wave vector in the in-plane direction of q_x=5.2 $\times 10^5$ cm^{-1} and with varying Bloch wave vector, q_z, in units of $q_z(a+b)$ for GaAs/AlAs MQW's of widths 40/6 and 40/80 Å . We have also calculated the dispersion curves for fixed q_x of 7.3 $\times 10^5$ cm^{-1} with varying q_z and they are virtually identical to those in Fig. 3. The analytical expressions for, and the derivation of, the dispersion relations of the GaAs and AlAs optical phonons are given in Refs. 13 and 27. For the 40/6 MQW, the AlAs barrier is two monolayers thick. There are only two confined modes in the AlAs energy region (upper part of [Fig. 3(a)], one of which mixes with the upper *interface* mode, plus the two *interface* modes. The modes which have the strongest interface components are those that show dispersion as the phonon wave vector in the growth direction is increased. Since the phonon modes have components in both in-plane and growth directions the *interface* modes are not purely symmetric or antisymmetric. For the 40/6 structure, the lower energy AlAs *interface* mode is more symmetric than the upper one. There are many more confined modes between the bulk GaAs LO (ω_{LO}) and TO (ω_{TO}) energies [lower part of Fig. 3(a)], since the well layers consist of 14 ML. As the Bloch wave vector q_z increases, some modes show strong dispersion. These are the MQW phonons, which are predominantly due to the upper and lower *interface*

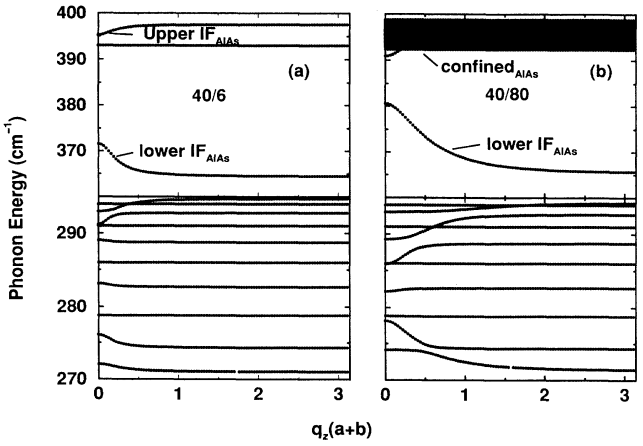

FIG. 3. Dispersions of the GaAs and AlAs optical phonons of the (40/6) and (40/80) GaAs/AlAs MQW's. A fixed in-plane phonon wave vector of $q_x \approx 5.2 \times 10^5$ cm^{-1} has been chosen. The dispersions are plotted against varying phonon wave vector in the growth direction q_z (in units of the MQW period).

modes. Since GaAs and AlAs are polar materials, the phonon modes have a scalar potential Φ associated with them. It is this scalar potential, or equivalently the electric field $\mathbf{E} = -\nabla\Phi$, that couples to the electrons by the Fröhlich interaction. The odd modes have an odd number of antinodes in the scalar potential across a particular well layer resulting in an overall macroscopic electric field, which has a finite value at a distance far from the individual well layer.[16,17] It is this electric field that interacts with the electric field of the interface modes to produce the anticrossings in the phonon dispersions. For the 40/6 structure, the modes with the strongest interface components are of mixed symmetry, but in this case, the upper mode is almost purely symmetric, while the lower mode is mostly antisymmetric at small values of $q_z(a+b) \approx 0.1$. It is the symmetric part of the phonon scalar potential that couples to the electrons in intrasubband transitions, since the electron wave functions have the same symmetry with respect to the center of the well.[26]

For the 40/80 sample there are 28 AlAs confined modes, which are found over a small energy range, due to the weak dispersion of bulk AlAs [upper part Fig. 3(b)]. These confined modes and their anticrossings with the upper *interface* mode cannot be resolved on the scale of Fig. 3. For this sample, the upper AlAs *interface* mode is much more symmetric than the lower AlAs *interface* mode. The GaAs optical-phonon modes for 40/80 are similar to those for 40/6, since the GaAs layer widths are the same. The dispersion coming from the contribution of the *interface* modes is now larger, since the ratio of the the GaAs and AlAs layer thicknesses is closer to unity. For this sample the lower GaAs *interface* mode is more symmetric than the upper GaAs *interface* mode, though the upper mode still has a significant symmetric part.

To estimate the strength of the electron-phonon interaction, we need to consider the magnitude of the scalar potential in the GaAs wells of the optical phonons involved in the electron relaxation. The value of the wave vector of the electron state in the growth direction before recombination will be similar to that of the initial created electron state, since we are considering intrasubband transitions. Thus, the wave vector transferred to the phonon in the growth direction is expected to be close to zero. To estimate the magnitude of the electron-phonon interaction, we take a small value of $q_z = 1.7 \times 10^5$ cm^{-1} [$q_z(a+b)$=0.085, for a=40 Å, b=20 Å]. We do not integrate the electron-phonon interaction over the Bloch wavector q_z, or in-plane wave vector q_x, though recombination with the same acceptor state and the fact that the Fröhlich interaction is $\propto \frac{1}{(q_x+q_z)^2}$ implies that interactions with phonons of small q_z and q_x will be strongly favored.

In order to determine the magnitude of the electron-phonon interaction for the individual phonon modes, it is necessary to obtain the value of the scalar potential of each mode in the GaAs well. The scalar potential, ϕ_{Ga}, of the GaAs modes for $0 \leq z \leq a$ is written as

$$\phi_{\mathrm{Ga}} = A_{\mathrm{norm}} \left[i \left(e^{iq_L z} + Be^{-iq_L z} \right) + s \left(Fe^{q_x z} + Ge^{-q_x z} \right) \right] e^{i(q_x x - \omega t)}, \quad (2)$$

which has been derived in Ref. 16, where the expressions for the constants A_{norm}, B, F, G, and s are also given. The phonon potential contains contributions from the longitudinal and interface components of the MQW optical phonons. q_L is the magnitude of the longitudinal part of the MQW phonon wave vector in the growth direction and q_x is the value of the phonon wave vector in the in-plane direction and also the magnitude of the MQW *interface* mode component in the growth direction. The phonon displacements contain additional contributions from the transverse modes, but due to the very weak electron-TO phonon interaction, the MQW phonon scalar potential has no bulk TO mode contribution. The AlAs phonons are confined to vibrate in the AlAs layers (along with the first Ga atoms in the well layers next to the interfaces, which also vibrate). However, in addition to the displacement and scalar potential in the AlAs layers, the AlAs modes have an associated scalar potential in the GaAs layers, which comes from the *interface* mode component of the optical phonons. This potential ϕ_{Al} is given by

$$\phi_{\mathrm{Al}} = A_{\mathrm{norm}} s \left(He^{q_x z} + Ie^{-q_x z} \right) e^{i(q_x x - \omega t)}, \quad (3)$$

where the appropriate constants for the AlAs modes are derived in Ref. 16. Using these expressions, we have determined the scalar potentials of the modes in the GaAs layers for fixed GaAs width of 40 Å and a number of different AlAs widths. The initial and final electron states are associated with the same confined level of the quantum well, so the Fröhlich interaction of this intrasubband transition couples to the part of the phonon scalar potential, which is symmetric with respect to the center of the well. We have calculated the value of the symmetric part of the scalar potential at the center of the well, $z = a/2$, with q_z=1.7 $\times$ 10 ^{5} cm^{-1} and q_x= 5.2 $\times$ 10^5 cm^{-1} for the optical-phonon modes. The modes with the largest potentials are those which have the largest interface contribution plus the 2nd confined mode of GaAs, LO_2. The magnitude of the scalar potential in the GaAs layers of the confined AlAs modes is a factor of 100 smaller. The value of the symmetric part of ϕ at the center of the GaAs layers for these significant modes is given in Fig. 4 for different barrier widths. At small barrier widths, the upper GaAs *interface* mode (asterisks) has the largest phonon potential, whereas for large barrier widths, the largest phonon potential is that of the upper AlAs *interface* mode (triangles). The magnitude of the confined LO_2 mode potential (circles) is almost independent of the barrier thickness and increases only slightly for large barriers, as some intermixing with the upper *interface* mode occurs.

From the magnitude of the phonon potentials, one would expect that the HPL spectra are dominated by GaAs phonons for small barrier widths and AlAs phonons for large barrier widths. To model the broad hot photoluminescence peaks ($\approx$ 200 cm^{-1}), we combine contributions centered at the GaAs and AlAs phonon frequencies and broaden them by a Gaussian distribution of full width at half maximum of 200 cm^{-1}. Since the Fröhlich interaction contribution to the HPL spectra is propor-

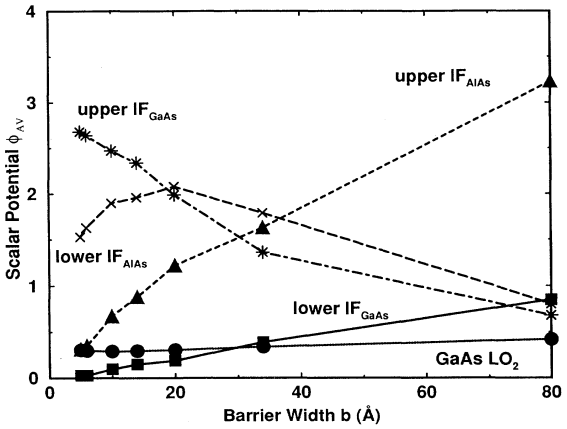

FIG. 4. The magnitude of the symmetric part of the phonon scalar potential at the center of the well layer for the MQW modes relevant to electron relaxation vs barrier width (b). The circles correspond to the GaAs LO_2 mode, the squares to the lower frequency GaAs interface mode, the triangles to the upper frequency AlAs interface modes, the crosses to the lower frequency AlAs interface mode, and the asterisks to the upper frequency GaAs interface mode.

tional to the square of the overlap integral of the subband wave functions with the phonon potential ϕ, the different relaxation paths have to be weighted by $(\phi_{Ga}/\phi_{Al})^2$, where ϕ_{Ga} is the sum for the scalar potentials of all the GaAs modes in Fig. 4 and ϕ_{Al} the sum of the two AlAs modes at a particular barrier width b. The peaks of the spectra, obtained in this way, are plotted as a function of barrier width in Fig. 2 (solid line). When the ratio$(\phi_{Ga}/\phi_{Al})^2$ is not too different from unity, as is the case for b=5 and 9 Å, the combination of these two contributions results in spectra with maxima at an energy between that of the GaAs and AlAs optical phonons. However, for b=80 Å, the ratio $(\phi_{Ga}/\phi_{Al})^2$ is only 0.15. The spectrum is dominated by the AlAs phonons and its maximun is centred at an energy very close to that of the strongest AlAs phonon mode. The calculation of the energy separation between the "0" and "1" phonon peaks of the HPL spectra agrees well with the experimental values in Fig. 2. The trend of increasing *effective* phonon energy with increasing barrier width is supported by the calculation. It is also interesting to observe that for b = 5 and 9 Å, the energy separation of the "0" and "1" phonon peaks is about 30 cm^{-1} larger than the energy of the GaAs phonons. This reflects the fact that although interaction with these modes is stronger, there is still a significant contribution from the AlAs phonons.

To simplify the calculation, we have not explicitly evaluated the electron-phonon interaction in the MQW's. If we had considered the decay of the electron wave functions into the AlAs barriers, then the interaction with the scalar potential of the phonon modes in the barrier would also contribute to the electron relaxation. This small effect would slightly increase the strength of interaction of the AlAs modes, compared to the GaAs modes and would, conceivably, give even better agreement for the effective energy of the emitted phonons when compared with the separation of the luminescence peaks in Fig. 2.

IV. CONCLUSIONS

Using hot-electron photoluminescence, we have investigated the relaxation of electrons in a series of GaAs/AlAs MQW's, with 40 Å well widths and barrier thickness between 5 Å and 80 Å . Due to the low density of the photoexcited electrons, their relaxation is accounted for by the emission of longitudinal optical phonons. Both sets of optical phonons at frequencies in the GaAs and AlAs reststrahl range contribute to the relaxation process for every sample. For the largest barrier width investigated, the energy of the emitted optical phonon is equal to the energy of the AlAs MQW phonon mode, which is a mixture of AlAs confined modes and the upper AlAs *interface* mode. The emission strength of a particular phonon mode is proportional to the square of the overlap integral of the phonon scalar potential with the initial and final electron states in the GaAs layers. For the case of intrasubband relaxation considered, electrons interact with the symmetric part of the phonon potential ϕ. For 80 Å barriers the ratio $(\phi_{Ga}/\phi_{Al})^2$ is 0.15, which accounts for the energy relaxation being dominated by the AlAs phonons. For small barriers, the emission of the GaAs modes is stronger. At a barrier width of b=5 Å, the ratio $(\phi_{Ga}/\phi_{Al})^2$ amounts to 2.5. The HPL oscillation period decreases to a value close to that of the GaAs optical phonons, nevertheless, there is still a significant contribution from the emission of AlAs modes. The calculated values of the effective energy of the emitted phonons agree quite well with the experiment.

ACKNOWLEDGMENTS

We thank H. Hirt, M. Siemers, and P. Wurster for technical assistance and J. Kuhl for a critical reading of the manuscript. V.F.S. and D.N.M. acknowledge financial support from the Volkswagen Foundation, the Russian Fund of Fundamental Investigations, the International Science Foundation (Grant No. R47000), and the Fonds der Chemische Industrie. V.F.S. acknowledges additional support from the Max-Planck-Gesellschaft, while M.P.C. is grateful to the European Union for financial support, to the Max-Planck-Institut for its hospitality and was at the latter stages self-supporting.

[1] D. N. Mirlin, I. Ja. Karlik, L. P. Nikitin, I. I. Reshina, and V. F. Sapega, Solid State Commun. **37**, 757 (1981).
[2] B. P. Zakharchenya, D. N. Mirlin, V. I. Perel, and I. I. Reshina, Usp. Fiz. Nauk **136**, 459 (1982) [Sov. Phys. Usp. **25**, 143 (1982)].
[3] B. P. Zakharchenya, P. S. Kop'ev, D. N. Mirlin, D. G. Polakov, I. I. Reshina, V. F. Sapega, and A. A. Sirenko, Solid State Commun. **69**, 203 (1989).
[4] R. G. Ulbrich, J. A. Kash, and J. C. Tsang, Phys. Rev. Lett. **62**, 949 (1989).
[5] G. Fasol, W. Hackenberg, H. P. Hughes, K. Ploog, E. Bauser, and H. Kano, Phys. Rev. B **41**, 1461 (1990).
[6] J. A. Kash, M. Zachau, M. A. Tischler, and U. Ekenberg, Phys. Rev. Lett. **69**, 2260 (1992).
[7] J. A. Kash, Phys. Rev. B **47**, 1221 (1993).
[8] C. L. Petersen, M. F. Frei, and S. A. Lyon, Phys. Rev. Lett. **63**, 2849 (1989).
[9] S. Baroni, P. Giannozi, and E. Molinari, Phys. Rev. B **41**, 3870 (1990).
[10] P. Giannozi, S. de Gironcoli, P. Pavone, and S. Baroni, Phys. Rev. B **43**, 7231 (1991).
[11] D. Strauch and B. Dorner, J. Phys Condensed Matter **2**, 1457 (1990).
[12] G. S. Spencer, J. Grant, R. Gray, J. Zolman, J. Menéndez, R. Droopad, and G. N. Maracas, Phys. Rev. B **49**, 5761 (1994).
[13] M. P. Chamberlain, M. Cardona, and B. K. Ridley, Phys. Rev. B **48**, 14 356 (1993).
[14] M. Zunke, R. Schorer, G. Abstreiter, W. Klein, G. Weimann, and M. P. Chamberlain, Solid State Commun. **93**, 847 (1995).
[15] A. J. Shields, M. Cardona, and K. Eberl, Phys. Rev. Lett. **72**, 412 (1994).
[16] A. J. Shields, M. P. Chamberlain, M. Cardona, and K. Eberl, Phys. Rev. B **51**, 17 728 (1995).
[17] A. Fainstein, P. Etchegoin, M. P. Chamberlain, M. Cardona, K. Tötemeyer, and K. Eberl, Phys. Rev. B **51**, 14 448 (1995).
[18] M. C. Tatham, J. F. Ryan, and C. T. Foxon, Phys. Rev. Lett. **63**, 1637 (1989).
[19] K. T. Tsen, K. R. Wald, T. Ruf, P. Y. Yu, and H. Morkoc, Phys. Rev. Lett. **67**, 2557 (1991).
[20] K. Huang and B. Zhu, Phys. Rev. B **38**, 13 377 (1988).
[21] E. Ozturk, N. C. Constantinou, A. Straw, N. Balkan, B. K. Ridley, D. A. Ritchie, E. H. Linfield, A. C. Churchill, and G. A. C. Jones, Semicond. Sci. Technol. **9**, 782 (1994).
[22] D. N. Mirlin, P. S. Kopév, I. I. Reshina, A. V. Rodina, V. F. Sapega, A. A. Sirenko, and V. M. Ustinov, in *Proceedings of the 22nd International Conference on the Physics of Semiconductors*, edited by D. J. Lockwood (World Scientific, Singapore, 1995), pp. 1288–1295.
[23] J. Kash, in *The Physics of Semiconductors* (Ref. 22), pp. 237–240.
[24] V. D. Dymnikov, V. I. Perel', and A. F. Polupanov, Fiz. Tekh. Poluprovodn. **16**, 235 (1982) [Sov. Phys. Semicond. **16**, 148 (1982)].
[25] U. Ekenberg, Phys. Rev. B **40**, 7714 (1989).
[26] M. Babiker, M. P. Chamberlain, and B. K. Ridley, Semicond. Sci. Technol. **2**, 582 (1987).
[27] M. P. Chamberlain and M. Cardona, Semicond. Sci. Technol. **9**, 749 (1994).